STEREOLOGICAL ANALYSIS OF THE GUINEA PIG PANCREAS

I. Analytical Model and Quantitative Description of Nonstimulated Pancreatic Exocrine Cells

ROBERT P. BOLENDER

From the Department of Anatomy, University of Berne, Berne, Switzerland

ABSTRACT

A stereological model which provides detailed quantitative information on the structure of the fasted, nonstimulated gland has been developed for the guinea pig pancreas. The model consists of morphologically defined space and membrane compartments which were used to describe the general composition of the tissue and the specific components of exocrine cells. The results are presented, where appropriate, relative to a cubic centimeter of pancreas, a cubic centimeter of exocrine cell cytoplasm, and to the volume of an average exocrine cell. The exocrine cells, accounting for 82% of the pancreas volume, consisted of 54% cytoplasmic matrix, 22% rough-surfaced endoplasmic reticulum (RER), 8.3% nuclei, 8.1% mitochondria, 6.4% zymogen granules, and 0.7% condensing vacuoles. Their total membrane surface area was distributed as follows: 60% RER, 21% mitochondria, 9.9% Golgi apparatus, 4.8% plasma membranes, 2.6% zymogen granules, 1.8% plasma membrane vesicles, and 0.4% condensing vacuoles. The application of this model to the study of membrane movements associated with the secretory process is discussed within the framework of an analytical approach.

INTRODUCTION

In recent years, the exocrine pancreas has been a subject of interest to cell biologists particularly with respect to the mechanisms of protein synthesis, intracellular transport, and discharge of secretory proteins (1–10). Although a considerable amount of biochemical data is now available, no attempt has been made to introduce stereological methods as an aid in the interpretation of studies concerned with the relationships of cellular ultrastructure to biochemical function. Consequently, the purpose of this paper is to provide detailed structural information on the pancreatic exocrine cells (ExC)[1] in the form of a stereological model designed to be compatible with biochemical studies. Within the framework of this model, an analytical approach to the study of cellular ultrastructure is described

[1] *Abbreviations used in this paper*: BaPM, basal plasma membrane; BaPMV, basal plasma membrane vesicles; BVW, blood vessel walls; CoV, condensing vacuoles; CyMa, cytoplasmic matrix; DC, duct cells; EExC, extra-exocrinocytic (nonexocrine) cells; EExS, extra-exocrinocytic spaces; EnC, endocrine cells; ExC, exocrine cells; ExCCy, exocrine cell cytoplasm; G, gland; GA, Golgi apparatus; IC, interstitial cells; IMiM, inner mitochondrial membrane; LaPM, lateral plasma membrane; LaPMV, lateral plasma membrane vesicles; LuPM, luminal plasma membrane; LuPMV, luminal plasma membrane vesicles;

which is currently being used to study the movements of ExC membranes during and after the secretion of zymogen.[2]

MATERIALS AND METHODS

Animals

Five male albino guinea pigs (BFA, Zurich, Switzerland) weighing 475–565 g (3–4 months old) were fasted overnight and a deep anesthesia was induced with Nembutal (sodium pentobarbital); they were maintained on NAFAG-830 (Gossau, Switzerland). The pancreas was rapidly removed from the animal, weighed[3] (after carefully removing adherent fat), and cut into five regions, equally long and designated A through E, beginning at the pancreas head and moving toward the tail. From the central portion of each region, blocks were removed and prepared for electron microscopy.

Electron Microscopy

Tissue blocks, 0.5 mm on a side, were fixed in 1% osmium phosphate buffer (340 mOsm) at pH 7.4 for 2 h at 0–4°C and stained *en bloc* with uranyl acetate (11). Tissue blocks were dehydrated by passing them through increasing concentrations of cold ethanol followed by propylene oxide, and were finally embedded in Epon (12). Sections, having an interference color of gray to silver (60–70 nm), were cut with a diamond knife on a Reichert ultramicrotome, mounted on 200 mesh grids having a carbon-coated parlodion film, and stained with lead citrate for 20 min (13). Micrographs were made on 35-mm film with Philips 200 and 300 microscopes, contact printed, and analyzed in a projector unit (14), which increases the primary magnification by approximately 10 ×. The magnification was determined by including a photograph of a calibration grating (E. F. Fullam Inc., Schenectady, N.Y.) on each film strip.

Mi, mitochondria; N, nuclei; NC, nerve cells; OMiM, outer mitochondrial membrane; PM, plasma membrane; PMV, plasma membrane vesicles; RER, rough-surfaced endoplasmic reticulum; SER, smooth-surfaced endoplasmic reticulum; S_V, surface density; V_V, volume density; ZG, zymogen granules.

[2] Bolender, R. P. 1974. Stereological Analysis of the guinea pig pancreas. II. Kinetics of the membranes and organelles in stimulated pancreatic exocrine cells. Manuscript in preparation.

[3] The specific gravity of the pancreas (1.08 g/cm^3) was determined by the method of Scherle (20); therefore, volume could be calculated from pancreas weight.

Stereological Model

The model for the guinea pig pancreas is outlined in Fig. 1. It shows how the pancreas was divided into morphologically defined components which have been quantitated by applying stereological methods. Essentially, the model has two major divisions: one the extra-exocrinocytic (nonexocrine) cells and spaces, and the other, the exocrine cells. The latter was divided into nuclear and cytoplasmic compartments following a scheme in which all the spaces and membranes of the exocrine cell cytoplasm were included within well defined compartments.[4] Wherever possible, these compartments were further subdivided in order to increase the sensitivity of the model.

A unique feature of the model is its analytical design. It allows one to account for all the cellular spaces and membranes within a unit volume or average cell. Consequently, a balance sheet can be constructed for experimental studies which makes it possible to detect changes within individual compartments or movements of material (spaces and membranes) from one compartment to another.

Three reference systems have been included in the model, a cubic centimeter of gland, a cubic centimeter of exocrine cell cytoplasm, and the volume and total membrane surface area of an average exocrine cell. The first two, using a unit volume, may be useful for comparisons with biochemical data related to a unit tissue weight (stereological volumes can be converted to weights when glandular density is known, see footnote 3). For mainly stereological studies, the average cell reference system is often preferable. It allows one to determine both absolute and relative values for most cellular compartments which, for the most part, will not be erroneously influenced by changes in cellular or tissue volume.

Morphological Criteria

Tissue and cellular components were identified on electron micrographs according to the following criteria.

Extra-Exocrinocytic Components

CELLS: Duct cells forming the tributaries of the duct system included centroacinar cells, and intra- and interlobular ducts (Fig. 2). Blood vessel walls included intrapancreatic arteries, veins, and capillaries, the latter being found most frequently (Fig. 3). Endocrine cells were found within islets and could be identified according to the morphology of their secretory granules (Fig. 4). Interstitial cells were found between acini and either displayed asymmetric

[4] The term "compartment" is defined as the aggregate of all the elements of a given component.

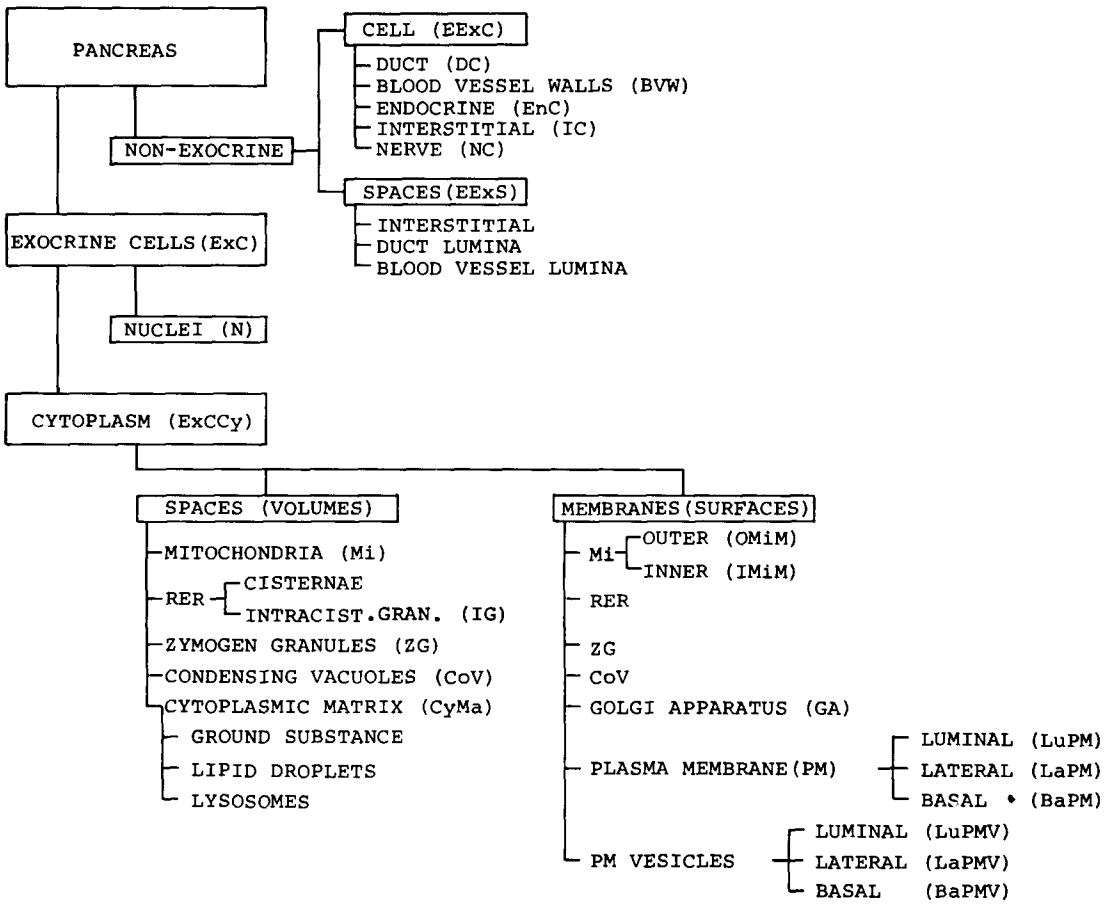

FIGURE 1 Stereological model of the pancreas.

nuclei surrounded by a scant cytoplasm or consisted of only cytoplasmic extensions (Fig. 5). Nerve cells consisted primarily of unmyelinated elements and were distinguished morphologically by the presence of a Schwann cell sheath and neurofilaments and spatially by their association to elements of the vascular system.

SPACES: Lumina of ducts, blood vessels, and interstitial areas were included within the extra-exocrinocytic space (Figs. 2 and 3); blood cells found within vessels were also counted as space.

EXOCRINE COMPONENTS

The basal portion of exocrine cells contained abundant rough-surfaced endoplasmic reticulum (RER) and, to a lesser extent, mitochondria and intracisternal granules (Figs. 6, 7), whereas the Golgi apparatus, condensing vacuoles, and zymogen granules were found in a more apical position (Figs. 8, 9). The plasma membrane was divided into three regions delimited by the apical tight junction and the basement membrane (Fig. 10). The luminal region began at the most apical part of the tight junction and included the plasma membrane and microvilli that face the lumen; the lateral region was found between the most apical part of the tight junction and the base of the cell where it first encounters the basement membrane; and finally, the basal region included the basal portion of the cell in contact with the basement membrane. Small, smooth-surfaced vesicles and tubules found just beneath the plasma membrane were identified according to the region in which they were found (Figs. 11–13). The vesicles appeared either "free" in the cytoplasm or continuous with the RER. The cytoplasmic matrix included the ground substance, Golgi apparatus, lipid droplets, lysosomes, and microperoxisomes.

Sampling

REGIONAL SAMPLING: For one animal in the series, six blocks (six micrographs per block) were chosen from each of the five regions, A–E, giving 36 micrographs per region and a total of 180 micrographs for

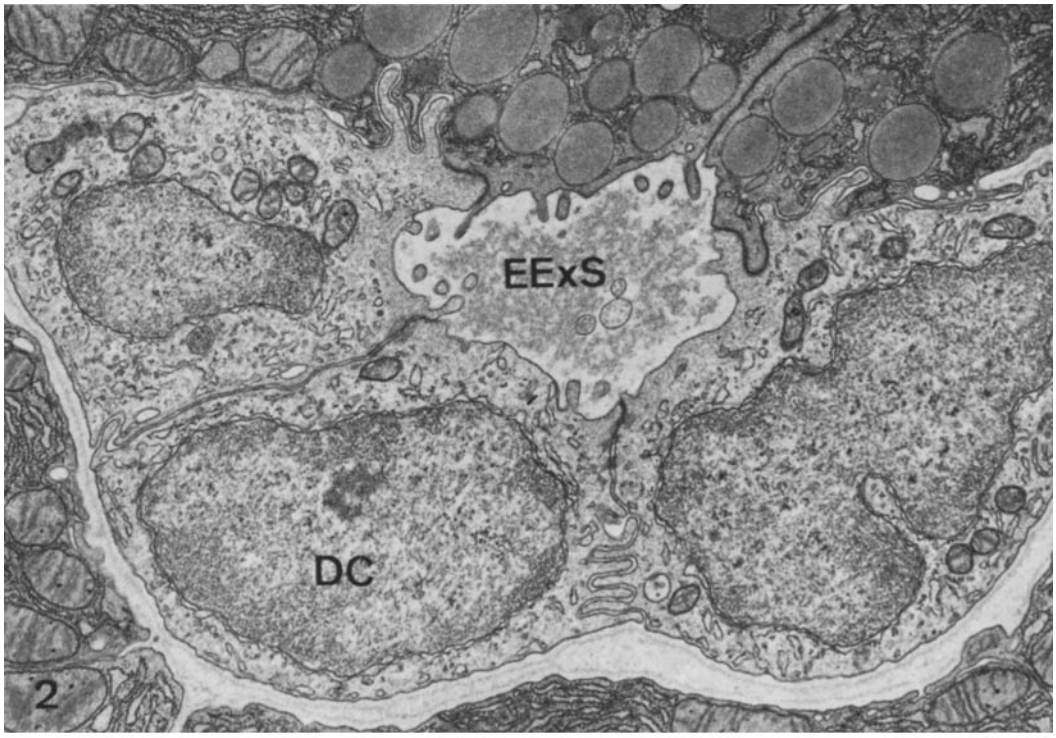

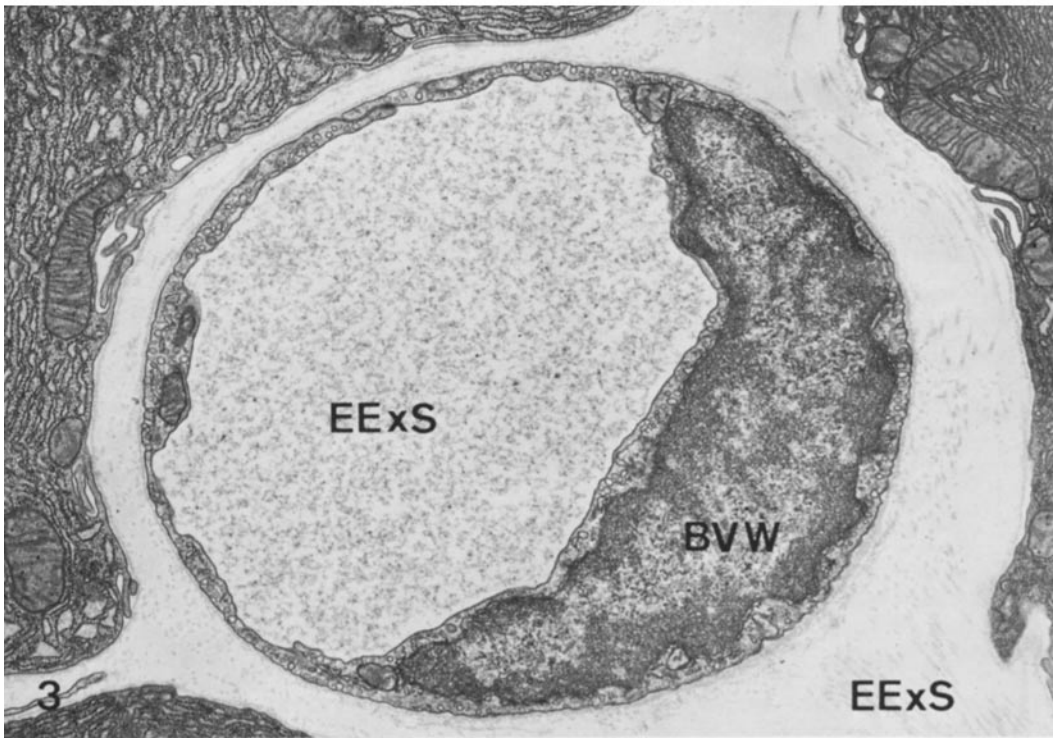

FIGURE 2 The duct cell (DC) compartment includes the centroacinar cells (represented here), plus intra- and interlobular ducts. Duct lumina are part of the extra-exocrinocytic space (EExS). × 15,000.

FIGURE 3 The cellular portions of the vascular elements (BVW) are included in this compartment (a capillary is illustrated). The vessel lumina and interstitial spaces are included with the extra-exocrinocytic space (EExS). × 13,000.

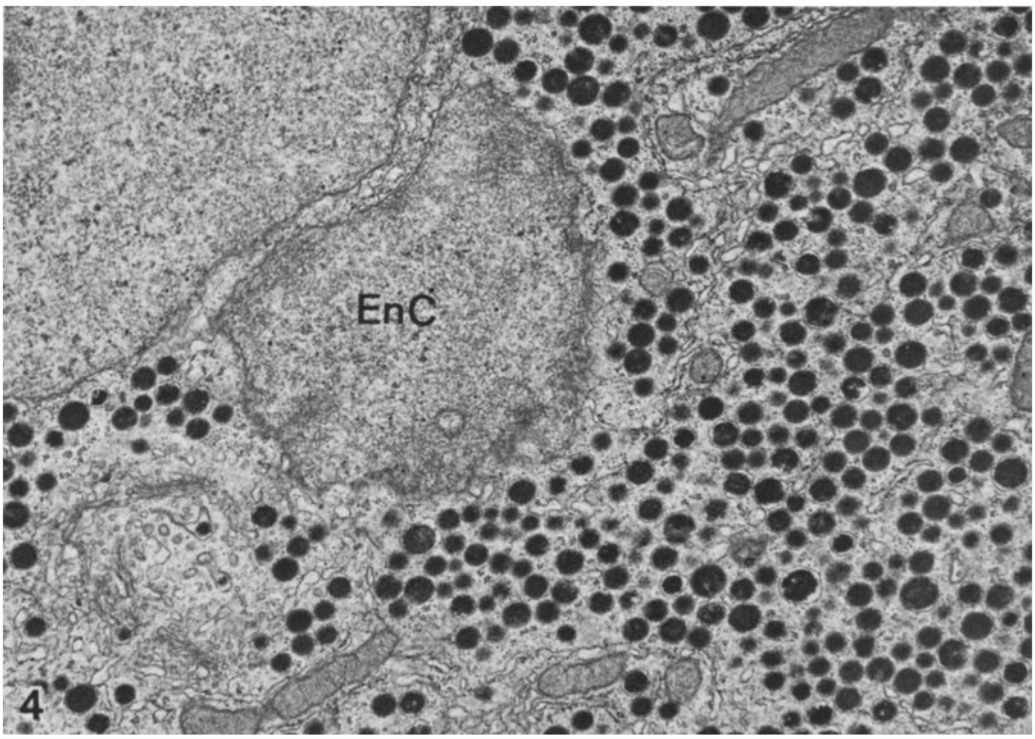

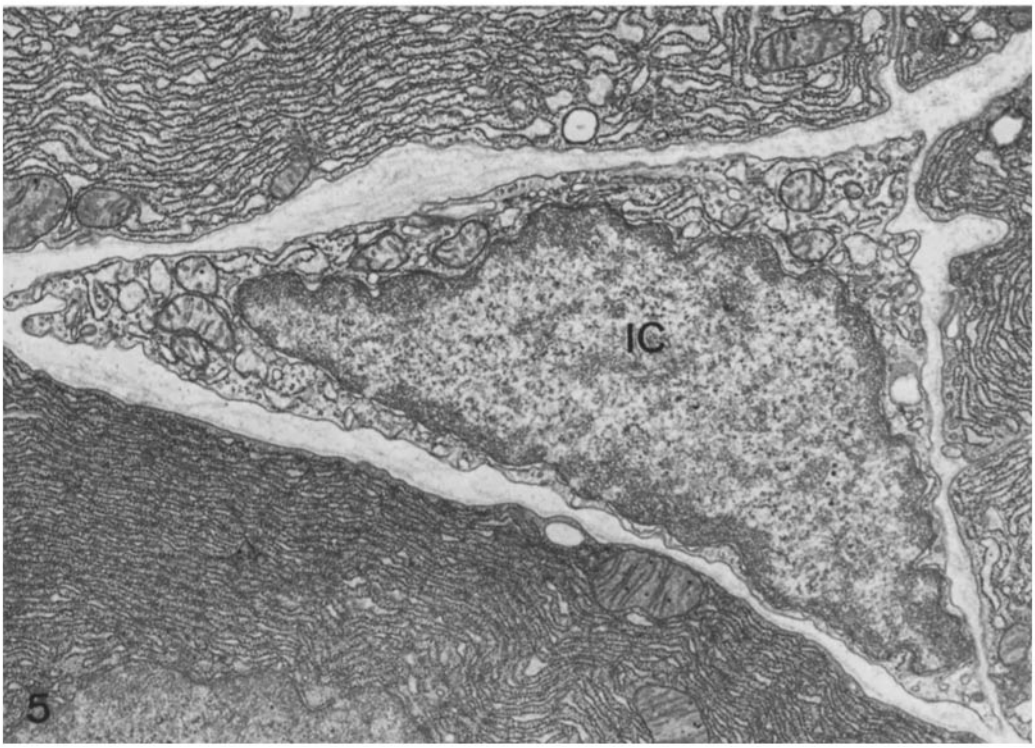

FIGURE 4 Endocrine cells (EnC) are found within islets and their cytoplasm contains granules typical of the cell type (an alpha cell is indicated). × 15,000.

FIGURE 5 Interstitial cells (IC) are found within the intercellular spaces and are characterized by their irregular nuclei and scant cytoplasm. × 15,000.

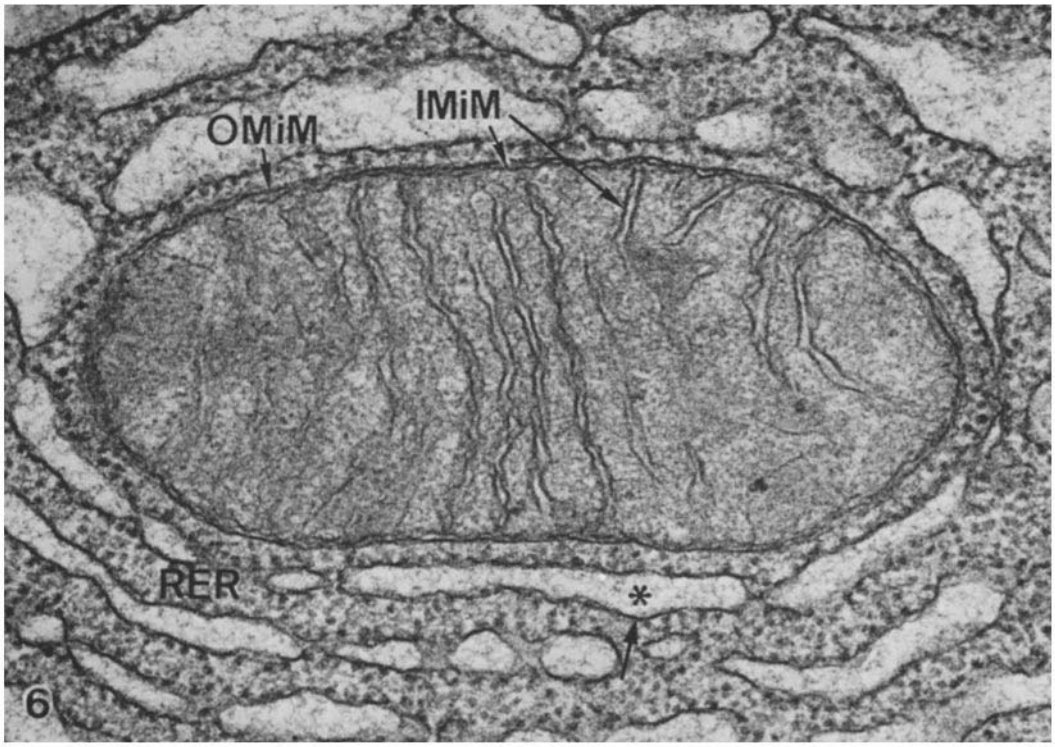

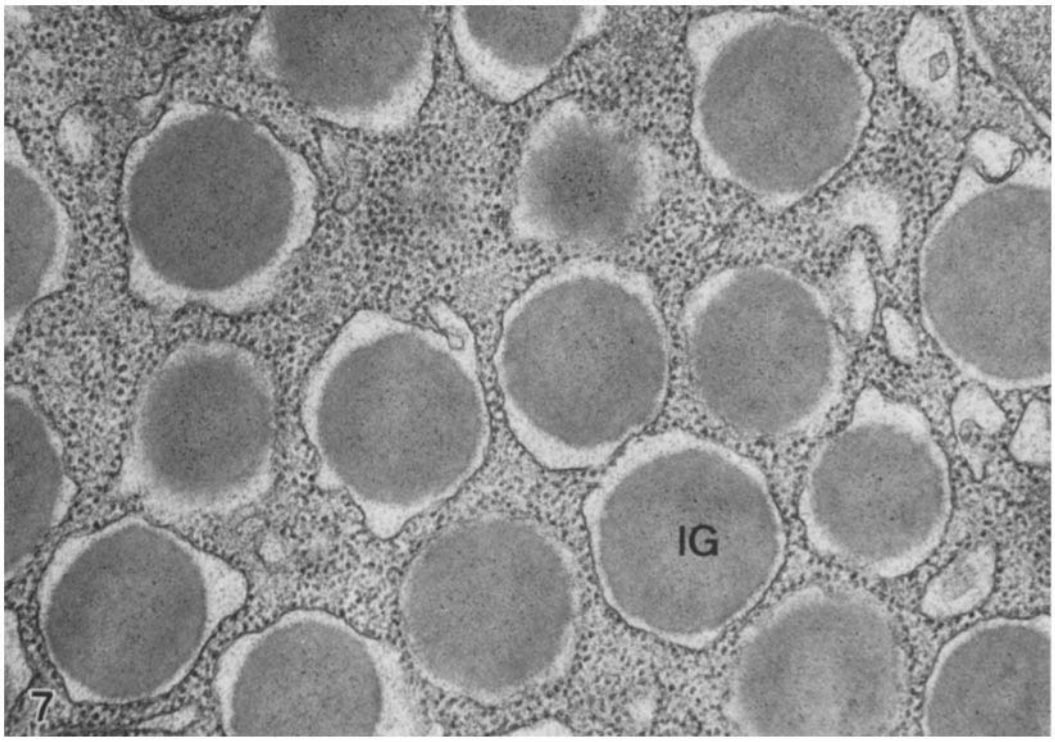

FIGURE 6 Inner and outer mitochondrial membranes (IMiM, OMiM) and the cisternal volume (*) and surface (arrow) of the RER are indicated. × 75,000.

FIGURE 7 Intracisternal granules (IG) are found within cisternae of the RER; they are not limited by a separate membrane. × 43,000.

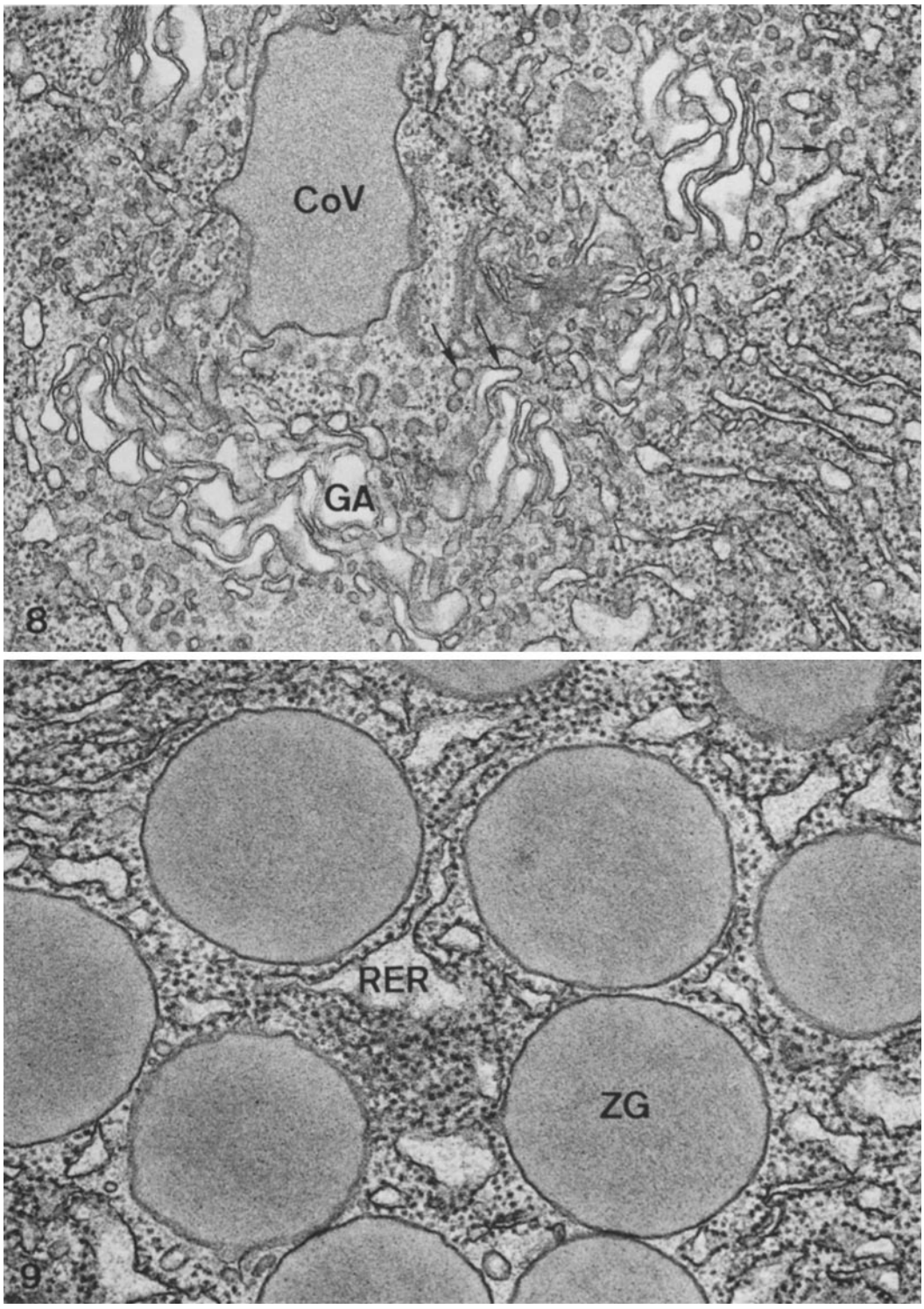

FIGURE 8 The Golgi apparatus (GA) includes cisternal and vesicular components (double arrow), as well as the transitional elements arising from the RER (single arrow); (SER was also counted with the GA). Condensing vacuoles (CoV) have irregular outlines and are associated with the GA. × 43,000.

FIGURE 9 Zymogen granules (ZG) surrounded by RER. × 59,000.

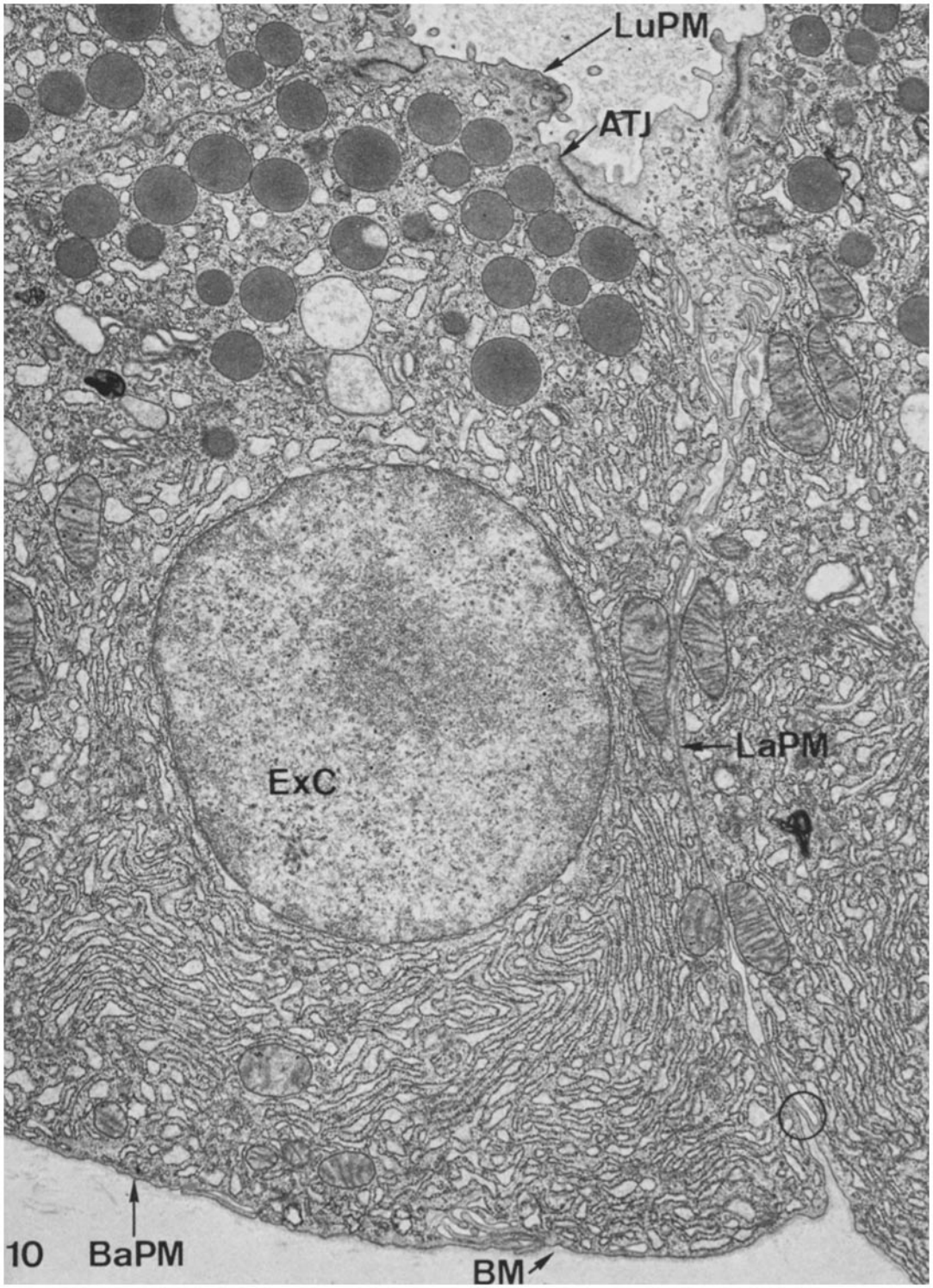

FIGURE 10 The plasma membrane of the exocrine cell (ExC) is divided into three regions according to the position of the apical tight junction (ATJ) and the basement membrane (BM): the luminal plasma membrane (LuPM) between two ATJ, the lateral plasma membrane (LaPM) from the ATJ to where the BM first comes in contact with the PM (circle), and the basal plasma membrane (BaPM) where the BM is adjacent to the PM.

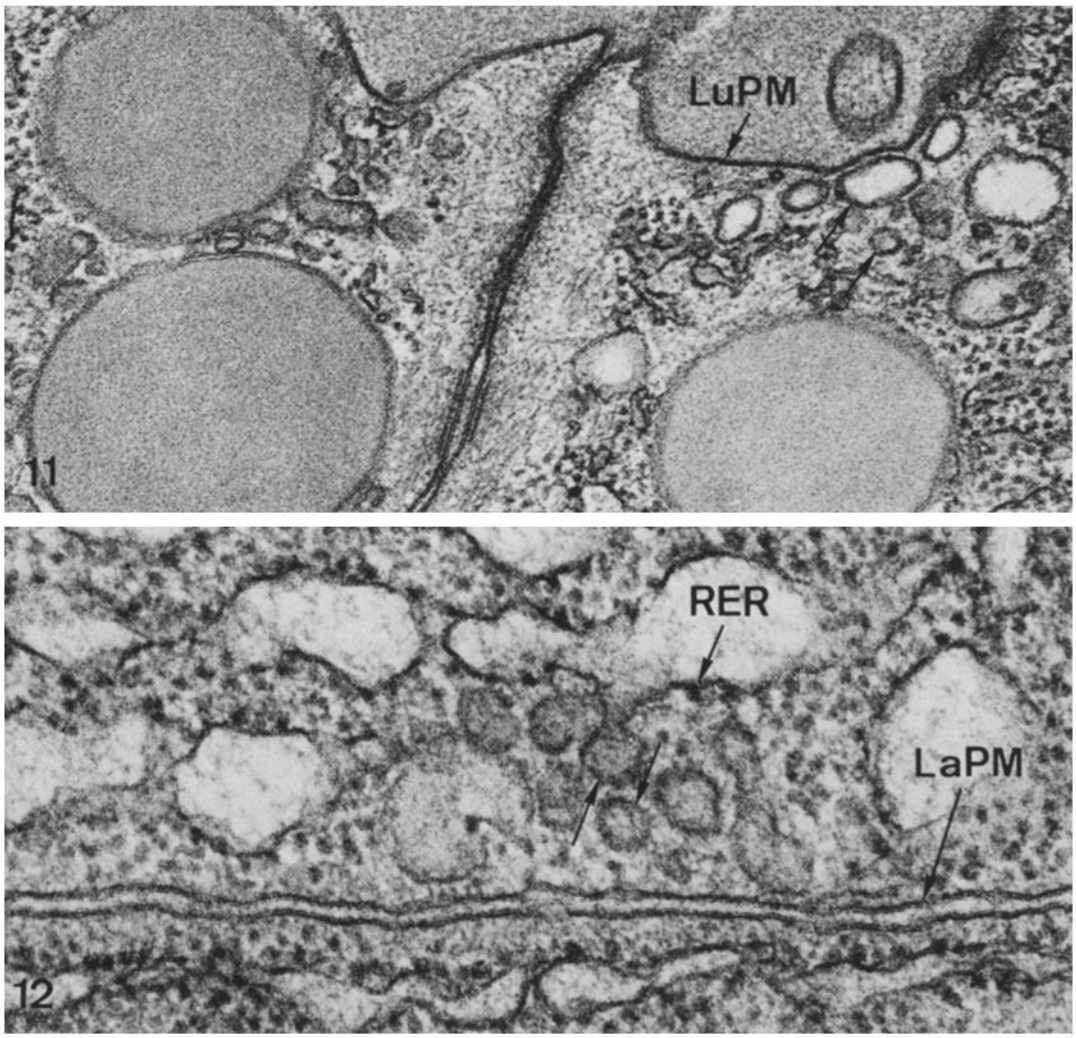

FIGURE 11 Luminal plasma membrane vesicles (arrows) are found adjacent to the luminal plasma membrane (LuPM). × 48,000.

FIGURE 12 Lateral plasma membrane vesicles (arrows) are found adjacent to the lateral plasma membrane (LaPM) and can be found to be continuous with the RER. × 110,000.

a single pancreas. Areas to be analyzed were selected according to a systematic sampling procedure (15). For each of the five regions, the mean and standard error were calculated for the number of points per micrograph falling on the different tissue components (see Table I, stage I), and the regions were compared by an analysis of variance test (16).

MULTIPLE STAGE SAMPLING (17): Since the components estimated at both the tissue and cellular levels represented a very broad range of sizes and frequencies, they could not be measured at a single magnification. Consequently, sampling was performed at several magnifications in order to establish adequate relationships between the size of the components being measured and the test systems. Table I lists the stages at which the various components were measured and includes the sampling area and linear probe length expressed per 100 micrographs.

Samples were collected in the following way. From each of five animals, 60 micrographs were selected per magnification stage. The set of micrographs for each animal came from five sections (12 micrographs per section) drawn from the five regions of the pancreas according to the following convention: region

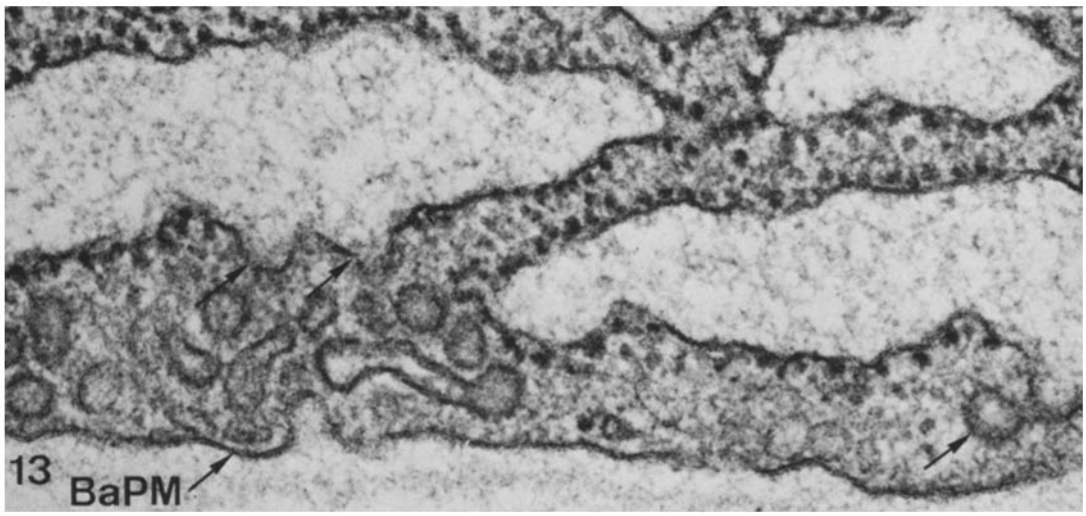

FIGURE 13 Basal plasma membrane vesicles and tubules are found adjacent to the basal plasma membrane (BaPM) which is identified by its association with the basement membrane. These smooth-surfaced vesicles are often found to be in connection with the RER (arrows). × 110,000.

A, 12 micrographs; B, 12; C, 12; D, 12; and E, 12; for a total of 60 micrographs. Areas to be analyzed were selected according to a systematic sampling procedure which consisted of photographing a single, randomly cut section on consecutive squares of a 200-mesh grid (17).

The sampling procedure and test systems applied to the three sampling stages were as follows.

STAGE I: Micrographs were made of sections filling entire grid squares, and a multipurpose test system (18) 27 × 27 cm, having a total number of 168 test points (P_T) with a point spacing of 2.2 cm, was used to estimate volume densities of the tissue components at × 6200 (Table I). This was the stage at which the mean nuclear diameter of exocrine cells was determined by measuring major and minor axes of nuclear profiles and then applying the Giger-Riedwyl procedure (19) to estimate the true size distribution of nuclei.

STAGE II: Micrographs were selected from the upper left corner of the grid square, and the multipurpose test system, already described for stage I, was used to estimate volume and surface densities at × 19,000 (Table I).

STAGE III: Micrographs were again selected from the upper left corner of the grid square, but this time a square lattice test system (1:9/36:324/4.5:1.5),[5] 27 × 27 cm, was used to estimate volume and surface densities at × 96,000 (Table I).

Stereological Procedures

Stereological estimates are expressed as densities which relate a volume, surface area, number, or length to a unit volume (e.g., 1 cm^3) of tissue. These densities, which are relative measurements, can either be used as such or related to an absolute tissue or nuclear volume. The tissue volume can be determined directly (20), whereas the nuclear volume must be calculated (14, 17). The latter calculation provides the volume of an average nucleus which, together with the nucleocytoplasmic volume ratio, can then be used to obtain average values for the cytoplasmic components with respect to an average "mononuclear" cell.

As mentioned in the section on sampling, several magnifications were required to measure the tissue and cellular elements. This meant, for the sake of convenience, that the estimates had to be related to different reference volumes. For instance, at stage I the cells were related to the volume of the pancreas, whereas at stages II and III, subcellular organelles were related to the cytoplasmic volume of exocrine cells. However, the stereological model was designed to relate the measures of exocrine cell components to a cubic centimeter of pancreas, to a cubic centimeter of exocrine cell cytoplasm, and to an average exocrine cell. The following stereological equations will show how this was accomplished.

STAGE I: The volume density of a glandular com-

[5] 1:9 signifies the ratio of coarse to fine points, 36:324 the number of coarse to fine points, and 4.5:1.5 the length in centimeters of one of the two linear probes (D, D') associated with each of the coarse and fine points.

TABLE I

Test System Characteristics for 100 Micrographs

Stage	Component	Sample area	Probe length (d)
		μm^2	μm
I	Exocrine cells Endocrine cells Duct cells Blood vessels Interstitial cells Nerve cells	1.796×10^5	
II	Cytoplasmic matrix Mitochondria Zymogen granules Condensing vacuoles Intracisternal granules	2.016×10^4	3.888×10^4
	Plasma membrane		3.888×10^4
III	Endoplasmic reticulum	7.955×10^2	1.663×10^3
	Golgi apparatus		4.989×10^3
	Outer mitochondrial membrane		1.663×10^3
	Inner mitochondrial membrane		1.663×10^3
	Plasma membrane vesicles		9.979×10^3

ponent i (V_{Vi}^{G})[6] was obtained by counting those points in the test system associated with i (P_i^G) in the underlying micrograph and those associated with the entire gland (P_T^G) according to Glagoleff (21) and as specified by Weibel et al. (18):

$$V_{Vi}^{G} = \frac{P_i^G}{P_T^G} \tag{1}$$

STAGE II: Volume densities were determined by counting only those points occurring within the exocrine cell cytoplasm (ExCCy), and were related to the gland (G) and average exocrine cell ($\overline{\text{ExC}}$) using the following formulas:

$$V_{Vi}^{\text{ExCCy}} = \frac{P_i^{\text{ExCCy}}}{P_T^{\overline{\text{ExCCy}}}} \tag{2}$$

$$V_{Vi}^{G} = \frac{P_i^{\text{ExCCy}}}{P_T^{\overline{\text{ExCCy}}}} \cdot V_{V\text{excey}}^{G} \tag{3}$$

$$V_i^{\overline{\text{ExC}}} = \frac{P_i^{\text{ExCCy}}}{P_T^{\overline{\text{ExCCy}}}} \cdot V_{\text{excey}}^{\overline{\text{ExC}}} \tag{4}$$

[6] Basic stereological notation is being used with the modifications introduced by Weibel (15). Lower case subscripts (i in the general case) identify the component (cf. Table III); the superscripts G, ExCCy, and $\overline{\text{ExC}}$ are introduced to identify the containing or reference space, i.e., whole gland, exocrine cell cytoplasm, or average exocrine cell, respectively.

where $V_{V\text{excey}}^{G}$ is the volume density of the ExCCy in the gland and $V_{\text{excey}}^{\overline{\text{ExC}}}$ is the volume of cytoplasm in an average exocrine cell. Surface densities were determined from counts of intersections (I_i) which occurred between linear probes of length d and membrane traces, plus counts of points falling on the exocrine cell cytoplasm. In using the multipurpose test system (15), the total length of the linear probe (L_T) was equal to one-half the number of test points (P_T) times d, the individual probe length. Hence, the stereological equation for estimating surface density (S_{Vi}) for this stage was:

$$S_{Vi} = \frac{2I_i}{L_T} = \frac{2I_i}{\frac{1}{2}P_T \cdot d} = \frac{4I_i}{P_T \cdot d} \tag{5}$$

and

$$S_{Vi}^{\text{ExCCy}} = \frac{4I_i^{\text{ExCCy}}}{P_T^{\overline{\text{ExCCy}}} \cdot d} \tag{6}$$

$$S_{Vi}^{G} = \frac{4I_i^{\text{ExCCy}}}{P_T^{\overline{\text{ExCCy}}} \cdot d} \cdot V_{V\text{excey}}^{G} \tag{7}$$

$$S_i^{\overline{\text{ExC}}} = \frac{4I_i^{\text{ExCCy}}}{P_T^{\overline{\text{ExCCy}}} \cdot d} \cdot V_{\text{excey}}^{\overline{\text{ExC}}} \tag{8}$$

STAGE III: The formulas used to estimate volume densities at stage III were similar to those applied at stage II, so they will not be repeated. However, the length of the linear probe (L_T) in the test system

used to estimate surface densities varied for different components, rarer ones requiring a greater length (see Table I). To accommodate these variations, a coherent test system (15) was used in which the length of the linear probe is flexible. Examples of the formulas used for the RER, GA, and PMV are given below to illustrate the variable (L_T):

$$S_{V_{rer}}^{ExCCy} = \frac{2I_{rer}^{ExCCy}}{P_T^{ExCCy} \cdot d} \quad (9)$$

where, for RER, $L_T = P_T^{ExCCY} \cdot d$

$$S_{V_{ga}}^{g} = \frac{2I_{ga}^{ExCCy}}{P_T^{ExCCy} \cdot 3d} \cdot V_{V_{excey}}^{g} \quad (10)$$

$$S_{pmv}^{\overline{ExC}} = \frac{2I_{pmv}^{ExCCy}}{P_T^{ExCCy} \cdot 6d} \cdot V_{excey}^{\overline{ExC}} \quad (11)$$

Calibration

The test systems contained linear probes of length D which were superimposed on the electron micrographs. When related to the nonmagnified specimen, the actual length of the linear probe (d) will depend on the length of the linear probe in the test system (D) and the micrograph magnification (M).

Each 35 mm film strip, which contained a set of pictures from a single animal taken at one magnification, was calibrated by micrographing a replica of a carbon grating having 21,600 spacings per centimeter (c). The number of spacings (n) per l centimeters on the projected image were counted and the length of D measured in centimeters. The actual length of d was determined by the following formula:

$$d = \frac{D \text{ (length of probe in test system)}}{M \text{ (magnification)}} \quad (12)$$

where $M = l \cdot c/n$.

Calculations

Stereological parameters were calculated for each animal using the total number of counts derived from 60 micrographs. The five animals were then used to calculate means and standard errors.

The point and intersection counts were collected with a data-recorder (22), and calculations were performed with a Hewlett-Packard 9100B programmable table top calculator.

RESULTS

Regional Sampling

As described in the methods section, samples were selected from five regions equally spaced along the longitudinal axis of the pancreas. This method of sampling was designed to detect variations within the pancreas in the volume density of the exocrine cells and, secondarily, those of the other tissue components. As shown in Fig. 14, the mean values of the exocrine cells for the five regions were quite similar with standard errors ~3.5% of the mean. Furthermore, an analysis of variance (Table II) showed that the samples of exocrine cells coming from the five regions belong to the same population. Although the variance analysis detected no regional differences between the remaining tissue components (Table II), Fig. 14 shows that the presence of a gradient for at least the rare endocrine and duct cells cannot be excluded on the basis of the current information.

Multiple-Stage Sampling

In Table III, morphological components of the guinea pig pancreas are characterized in terms of volumes and surface areas and, wherever appropriate, these parameters are related to the volumes of the pancreas, exocrine cell cytoplasm, and average exocrine cell. The upper portion of this table characterizes the tissue and extracellular components as volume densities according to the model of Fig. 1. The relative amounts of these components are represented graphically in Fig. 15, where they are expressed as a percent of the pancreas volume. It can be seen that the exocrine cells account for 82.1% of this volume (89.7% of the total cellular compartment, spaces not included) with only 9.6% coming from other cell types and 8.4% from the extracellular spaces.

The remainder of Table III characterizes the components of exocrine cells either as volumes or surface areas. A portion of these values are summarized in Figs. 16 and 17, where they are expressed as a percent of the total volume or membrane surface area of the exocrine cells. It can be seen in Fig. 16 that the cytoplasmic matrix was the major cytoplasmic component accounting for 54.3% of the cell volume. Of the remaining components, the volume of the RER cisternae contributed 21.8%, while the nuclei, mitochondria, and zymogen granules provided 8.3%, 8.1%, and 6.4%, respectively. Finally, the condensing vacuoles and intracisternal granules were found to be rare components, adding only 0.7% and 0.4% to the volume.

The surface density of the exocrine cell membranes is presented in a similar way in Fig. 17. The

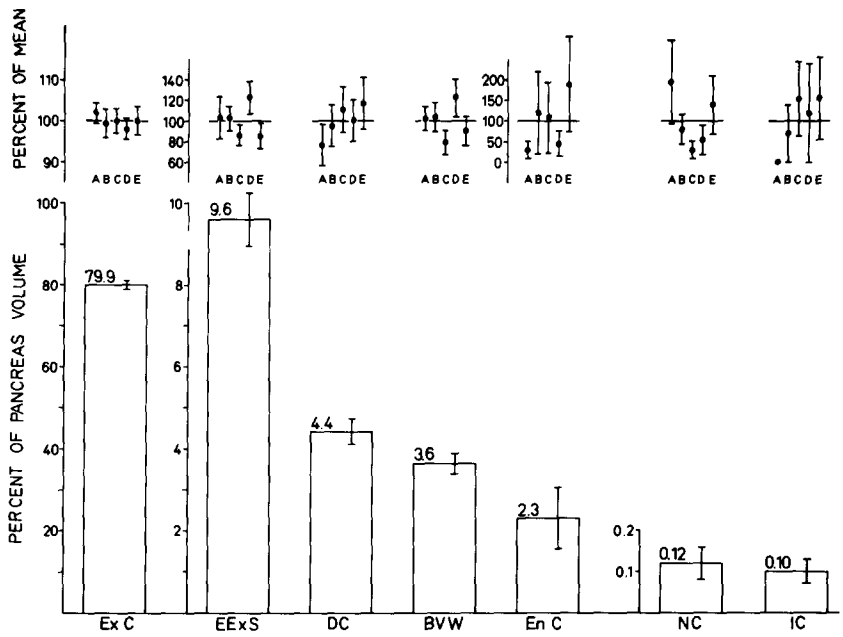

FIGURE 14 The upper portion of the graph shows the variation in the estimates for the tissue components coming from five regions of a single pancreas, designated A–E. The value for each region is expressed as a percent of the mean derived from the five regions. This mean is given beneath the regional values and is expressed as a percent of the pancreas volume. Standard errors are indicated.

TABLE II

Analysis of Variance for Points Falling on Tissue Components

Region	P_{exc}	P_{eexs}	P_{dc}	P_{bvw}	P_{enc}	P_{nc}	P_{ic}
A	124.25	16.667	5.694	6.250	1.222	0.389	0.000
	3.38	*3.128*	*1.533*	*0.703*	*0.771*	*0.196*	*0.000*
B	120.58	16.500	7.000	6.389	4.917	0.167	0.111
	4.52	*2.014*	*1.405*	*0.829*	*4.055*	*0.075*	*0.111*
C	122.36	13.861	8.194	4.917	4.306	0.056	0.250
	3.92	*1.764*	*1.624*	*0.742*	*3.362*	*0.039*	*0.146*
D	118.72	19.806	7.333	7.556	1.889	0.111	0.194
	3.27	*2.604*	*1.504*	*1.075*	*1.200*	*0.066*	*0.194*
E	120.92	13.750	8.611	5.556	7.611	0.278	0.250
	4.66	*1.782*	*1.935*	*0.852*	*4.616*	*0.136*	*0.161*
F ratio	0.27	1.15	0.50	1.36	0.64	1.31	0.58
F.95 (4,175)	2.43	2.43	2.43	2.43	2.43	2.43	2.43

The mean number of points coming from 36 micrographs with standard errors of the mean (italicized) are indicated for each sampling region. Exocrine cells (exc), extra-exocrinocytic spaces (eexs), duct cells (dc), blood vessel walls (bvw), endocrine cells (enc), nerve cells (nc), and interstitial cells (ic) are included.

total surface area of the exocrine cell membranes in the pancreas was 10.4 m^2/cm^3 or 9.6 m^3/g. To this amount, the RER contributed 59.9%, but considerably more (76.6%) when the membranes associated with mitochondria were excluded from the calculation.

No attempt was made to include a separate smooth-surfaced endoplasmic reticulum (SER) category in the model because it was not always possible to discriminate between SER and other smooth-surfaced membranes (transition elements and vesicles) found at the periphery of the Golgi

TABLE III

Normal Guinea Pig Pancreas (Uncorrected for Systematic Errors)

Component	Parameter	Symbol	Density per 1 cm³ gland*	Density per 1 cm³ exocrine cell cytoplasm	Units	Value per average exocrine cell	Units
Animal	Weight	W_{gp}	520.00		g		
			17.61				
Pancreas	Volume	V_p	1.22		cm^3		
			0.10				
Extra-exocrinocytic spaces	Volume	V_{eexs}	0.0838		cm^3/cm^3		
			0.0095				
Extra-exocrinocytic cells	Volume	V_{eexc}	0.0956		cm^3/cm^3		
Duct cells	Volume	V_{dc}	0.0393		cm^3/cm^3		
			0.0023				
Blood vessel walls	Volume	V_{bvw}	0.0368		cm^3/cm^3		
			0.0025				
Endocrine cells	Volume	V_{enc}	0.0177		cm^3/cm^3		
			0.0049				
Interstitial cells	Volume	V_{ic}	0.0010		cm^3/cm^3		
			0.0004				
Nerve cells	Volume	V_{nc}	0.0008		cm^3/cm^3		
			0.0001				
Exocrine cells	Volume	V_{exc}	0.8207		cm^3/cm^3	1060.00	μm^3
						84.78	
Nuclei	Volume	V_n	0.0738		cm^3/cm^3	106.50	μm^3
			0.0014			*7.16*	
Cytoplasm	Volume	V_{cy}	0.7469	1.0000	cm^3/cm^3	953.60	μm^3
			0.0071			*78.73*	
Zymogen granules	Volume	V_{zg}	0.0568	0.0692	cm^3/cm^3	65.24	μm^3
			0.0048	*0.0052*		*6.01*	
	Surface	S_{zg}	2728.0	3332.5	cm^2/cm^3	317.30	μm^3
			115.0	*132.5*		*28.88*	
Condensing vacuoles	Volume	V_{cov}	0.0066	0.0080	cm^3/cm^3	7.42	μm^2
			0.0007	*0.0008*		*0.52*	
	Surface	S_{cov}	422.50	513.60	cm^2/cm^3	49.03	μm^2
			56.69	*64.36*		*8.40*	
Intracisternal granules	Volume	V_{ig}	0.0036	0.0043	cm^3/cm^3	3.64	μm^3
			0.0018	*0.0021*		*1.80*	
Mitochondria	Volume	V_{mi}	0.0724	0.0884	cm^3/cm^3	83.63	μm^3
			0.0037	*0.0044*		*6.42*	
Outer mitochondrial membrane	Surface	S_{omim}	3924.0	4803.0	cm^2/cm^3	460.50	μm^2
			173.4	*242.5*		*48.00*	
Inner mitochondrial membrane	Surface	S_{imim}	17560.0	23490.0	cm^2/cm^3	2238.0	μm^2
			702.5	*811.9*		*204.3*	
Rough-surfaced endoplasmic reticulum	Volume	V_{rer}	0.1947	0.2605	cm^3/cm^3	249.30	μm^3
			0.0080	*0.0087*		*25.08*	
	Surface	S_{rer}	62210.0	83310.0	cm^2/cm^3	8047.0	μm^2
			3312.0	*4517.0*		*974.0*	
Golgi apparatus	Surface	S_{ga}	10270.0	13770.0	cm^2/cm^3	1270.0	μm^2
			1794.0	*2424.0*		*183.9*	
Cytoplasmic matrix	Volume	V_{cyma}	0.4844	0.5697	cm^3/cm^3	544.30	μm^3
			0.0050	*0.0110*		*48.62*	

TABLE III—(*Continued*)

Component	Parameter	Symbol	Density per 1 cm³ gland*	Density per 1 cm³ exocrine cell cytoplasm	Units	Value per average exocrine cell	Units
Plasma membrane	Surface	S_{pm}	4965.00	6073.0	cm^2/cm^3	581.9	μm^2
			78.46	*145.7*		*55.6*	
Luminal plasma membrane	Surface	S_{lupm}	239.66	296.30	cm^2/cm^3	28.85	μm^2
			57.50	*74.88*		*8.40*	
Lateral plasma membrane	Surface	S_{lapm}	3333.0	4073.0	cm^2/cm^3	388.70	μm^2
			100.3	*102.9*		*33.57*	
Basal plasma membrane	Surface	S_{bapm}	1392.00	1704.0	cm^2/cm^3	164.40	μm^2
			74.56	*104.7*		*20.42*	
Plasma membrane vesicles	Surface	S_{pmv}	1866.0	2495.0	cm^2/cm^3	239.00	μm^2
			193.7	*252.2*		*33.78*	
Luminal vesicles	Surface	S_{lupmv}	272.00	361.60	cm^2/cm^3	36.33	μm^2
			70.01	*89.81*		*11.30*	
Lateral vesicles	Surface	S_{lapmv}	519.20	693.2	cm^2/cm^3	64.79	μm^2
			85.27	*111.3*		*10.81*	
Basal vesicles	Surface	S_{bapmv}	1074.0	1440.0	cm^2/cm^3	137.90	μm^2
			161.6	*220.9*		*24.58*	

Standard errors of the mean values are italicized.
* Does not apply to animal weight and pancreas volume.

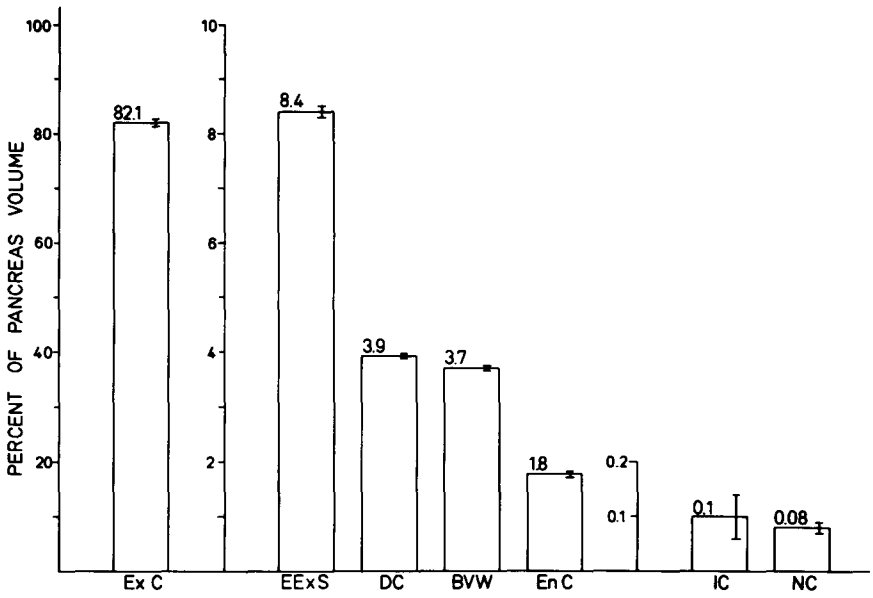

FIGURE 15 Tissue components of the pancreas are expressed as a percent of the total glandular volume. The means and standard errors are derived from five animals.

apparatus. However, a rough estimate for a "contaminated" SER was found to be $<1\%$ of the total membrane surface area.

The mean diameter of exocrine cell nuclei, derived from 2300 profiles taken from five animals, was 5.34 ± 0.1 μm, which gave a mean nuclear volume of 106.5 ± 7.2 μm^3. Using this absolute value and the relative nucleo-cytoplasmic volume

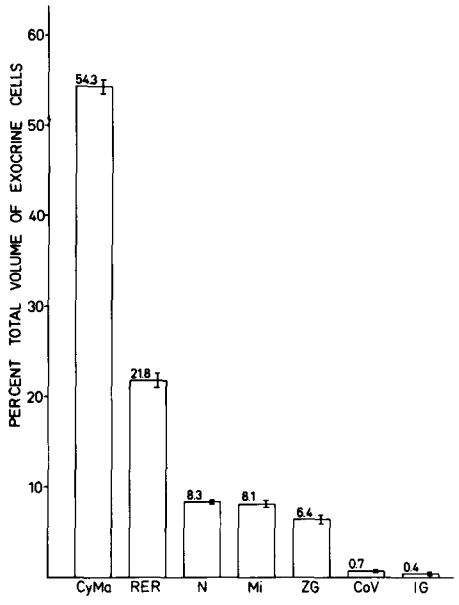

FIGURE 16 The volumes of the exocrine cell (ExC) components are expressed as a percent of the total volume of ExC. Standard errors of the mean are indicated.

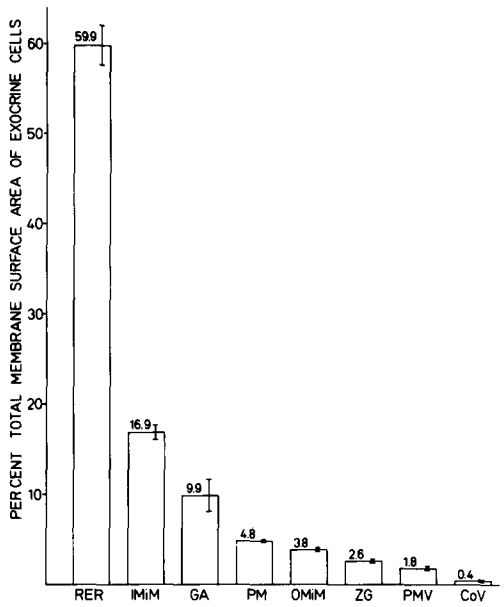

FIGURE 17 The surfaces of exocrine cell (ExC) components are given as a percent of the total membrane surface area of ExC. Standard errors are indicated.

ratio, absolute values were calculated for all the components of the exocrine cells in terms of an "average cell." This "cell" had a volume of 1060 μm^3 and a total membrane area of 13,200 μm^2 (Table III).

DISCUSSION

Evaluation of Methods

FIXATION: During the course of this study and the former one on the liver (11), it has become increasingly apparent that the choice of an adequate procedure for tissue fixation is of considerable importance in performing stereological techniques. The identification of cellular structures as well as the collection of data from electron micrographs was greatly facilitated by using a standardized fixation procedure and *en bloc* staining, which increased the contrast of the cellular membranes. Under these conditions, one could assign more exact morphological characteristics to cellular components which were, in turn, easier to recognize.

SAMPLING: An analysis of variance applied to a single animal, sampled from five representative regions, has provided evidence that the pancreas is homogeneous throughout with respect to the exocrine cells sampled at the tissue level. Therefore, it is concluded that a representative sample of exocrine cells can be drawn from anywhere within the pancreas. It should be noted, however, that although no differences between tissue components could be detected by the analysis, certain rare components occurring in clusters (for example, duct and endocrine cells) were, most likely, not sufficiently sampled to rule out the possibility of a tissue gradient.

In determining the stereological parameters of this study, an excessive number of micrographs were used because a large amount of data were available. However, the most efficient way to use stereological techniques is to determine the sample size required to fulfill the conditions of representativeness at each sampling level. The advantage of this procedure is that for many parameters the number of counts can be substantially reduced. On the other hand, when dealing with rare components, it may be necessary to increase the sample size. In either case, it is important to know whether or not the sample size one has chosen is representative of the tissue or cell population being measured. An in-depth study of the problems of sampling the guinea pig pancreas for stereological analysis is being prepared.

TEST SYSTEMS: The test systems were chosen to measure components with a minimum amount of

work. For volume estimates, the point density was arranged according to conventions proposed by Hilliard and Cahn (23) and by Weibel (15). This amounted to adjusting the primary magnifications of the films so that when projected onto the test systems, roughly one point fell on the component being measured; the above references can be consulted for details.

The fitting of magnifications to test systems for estimating surface densities is not so well defined (15, 24). Consequently, an empirical technique was used which consisted of first choosing a magnification at which the membranes under consideration could be easily identified and then applying a test system to the micrographs which made frequent intersections with the membranes. The length of the linear probe could then be reduced as long as doing so did not affect the estimates. Although this procedure appeared to be adequate, a more systematic consideration of the relationship of membrane density to linear probe density is needed.

Discussion of Results

The dimensions of an average exocrine cell were smaller than a comparable hepatocyte (11, 17). Exocrine cell volume (1060 μm^3) was approximately one-fifth that of the hepatocyte (4940 μm^3). The exocrine cell nuclear and cytoplasmic compartments contained 106 μm^3 and 954 μm^3, whereas the hepatocyte was larger with 300 μm^3 and 4640 μm^3; mitochondrial volumes were 84 μm^3 and 1170 μm^3, respectively. Similarly, the surface area of membranes was generally smaller in the exocrine cell: 8047 μm^2 vs. 37,900 μm^2 for the RER and 2699 μm^2 vs. 42,250 μm^2 for mitochondria; there were, however, 1270 μm^2 vs. 390 μm^2 for the Golgi apparatus.

Biochemical studies have suggested that after the release of secretory proteins from granules by the process of exocytosis, the membrane brought to the luminal surface of the pancreas is returned to the cellular interior and thought to be reutilized in the formation of new secretory granules (7–10). On the other hand, studies on the rat parotid gland conclude that the membrane protein of the secretory granules is not reused, rather it is synthesized *de novo* along with new secretory granules (25). In both cases, however, it is agreed that the membrane added to the plasma membrane during exocytosis is subsequently removed. The mechanism by which this withdrawal occurs is still unknown, but it has been suggested that it may be brought about by the internalization of intact membrane patches (1) or by membrane degradation at the molecular level (26).

If the granule membrane is transferred from the plasma membrane to the cytoplasm in intact patches, then under the proper experimental conditions it should be possible to detect this inward movement using the stereological model. The best of the morphological candidates for the internalized membrane are the plasma membrane vesicles (PMV) which have been included as a subdivision of the more general smooth membrane compartment in order to consider the role they might play in this process. These vesicles have been implicated by a number of authors as representing, either in part or totally, internalized granule membrane (1, 25). This suggestion of an inward movement of membranes has been confirmed at the lateral and basal surfaces of the exocrine cell by our preliminary experiments with ferritin (unpublished), and by those of Geuze and Poort (27). It should be pointed out, however, that even after an approximate correction is applied for section thickness (unpublished method of Weibel), the surface area of the PMV ($\sim$1250 cm^2/cm^3) represents about 40% of the ZG membranes ($\sim$3000 cm^2/cm^3). In order to account for PMV coming from zymogen granule membrane previously brought to the cellular surface by exocytosis, it would be necessary to postulate a spontaneous release of zymogen granules amounting to about one-third of the granule compartment. This requirement is not supported by either morphological or biochemical data coming from the nonstimulated pancreas. The morphological data would lead to the conclusion, therefore, that if the PMV do represent internalized PM, and if the vesicles do not accumulate, then the PM would have to acquire membrane from a source additional to the ZG to account for the surface area of the PMV compartment.

The stereological model for the pancreas represents an improvement over descriptive morphology in that it provides quantitative information on the volumes and surface areas of cellular components. In attempting to relate morphological to biochemical data, however, problems arise because comparisons are usually indirect. This results from the fact that morphological changes in intact tissue are being compared to biochemical fractions that represent only a portion of the total tissue. The quality of the comparison, consequently,

will depend on how closely the membranes and organelles of the fractions, which contain, for example, structural components characterized by marker enzymes, represent the corresponding components in the intact tissue. A more direct relationship between structure and function might be obtained by extending the stereological determinations to the homogenate and fractions and then analyzing both morphological and biochemical data within a coordinated analytical framework (28). This approach would allow one to relate biochemical data to membrane surface area and organelle volume, thereby avoiding the problems associated with protein and phospholipid reference systems.

Nevertheless, the model in its present form contains considerable information for biochemists. It allows one to determine from intact tissue relative amounts of individual membranes within a total membrane compartment, or subcompartment. For example, a microsomal fraction containing just RER and Golgi membranes would be expected to contain 86% rough- and 14% smooth-surfaced membranes if the fraction was representative of intact exocrine cells. Likewise, a representative granule preparation would contain 87% zymogen granule membranes and 13% condensing vacuole membranes; similar comparisons can be made for organelle volumes. Of course, these comparison will be more meaningful when analytical fractionation techniques are used.

In conclusion, detailed morphological data on exocrine cells of the guinea pig pancreas have been presented within the framework of an analytical model. Reference systems have been included that allow one to detect structural changes in cells and to make comparisons with biochemical data. Currently, the model is being used to study the movements of spaces and membranes during the secretory cycle. It is hoped that this approach will provide new insights into the morphological role of membranes in the synthesis, intracellular transport, and release of secretory proteins.

I wish to thank Dr. E. R. Weibel for his many helpful suggestions and Mrs. Margaret Fehlmann-Küenzi, Mrs. Rosmarie Bachmann, Mr. Karl Babl, and Mrs. Esther Hassler for their expert technical assistance.

This work was supported by grant no. 3.554.71 from the Swiss National Science Foundation, and by grants from the Leopold Schepp Foundation and the American-Swiss Foundation.

Received for publication 2 August 1973, and in revised form 19 December 1973.

REFERENCES

1. PALADE, G. E. 1959. Functional changes in the structure of cell components. *In* Subcellular Particles. T. Hayashi, editor. Ronald Press Company, New York. 64.
2. CARO, L. G., and G. E. PALADE. 1964. Protein synthesis, storage, and discharge in the pancreatic exocrine cell; an autoradiographic study. *J. Cell Biol.* **20**:473.
3. HOKIN, L. E. 1968. Dynamic aspects of phospholipids during secretion. *Int. Rev. Cytol.* **23**:187.
4. JAMIESON, J. D., and G. E. PALADE. 1967. Intracellular transport of secretory proteins in the pancreatic exocrine cell. I. Role of the peripheral elements of the Golgi complex. *J. Cell Biol.* **34**:577.
5. JAMIESON, J. D., and G. E. PALADE. 1967. Intracellular transport of secretory proteins in the pancreatic exocrine cell. II. Transport to condensing vacuoles and zymogen granules. *J. Cell Biol.* **34**:597.
6. JAMIESON, J. D., and G. E. PALADE. 1971. Synthesis, intracellular transport, and discharge of secretory proteins in stimulated pancreatic exocrine cells. *J. Cell Biol.* **50**:135.
7. MELDOLESI, J., J. D. JAMIESON, and G. E. PALADE. 1971. Composition of cellular membranes in the pancreas of the guinea pig. I. Isolation of membrane fractions. *J. Cell Biol.* **49**:109.
8. MELDOLESI, J., J. D. JAMIESON, and G. E. PALADE. 1971. Composition of cellular membranes in the pancreas of the guinea pig. II. Lipids. *J. Cell Biol.* **49**:130.
9. MELDOLESI, J., J. D. JAMIESON, and G. E. PALADE. Composition of cellular membranes in the pancreas of the guinea pig. III. Enzymatic activities. *J. Cell Biol.* **49**:150.
10. MELDOLESI, J., and D. COVA. 1972. Composition of cellular membranes in the pancreas of the guinea pig. IV. Polyacrylamide gel electrophoresis and amino acid composition of membrane proteins. *J. Cell Biol.* **55**:1.
11. BOLENDER, R. P., and E. R. WEIBEL. 1973. A morphometric study of the removal of phenobarbital-induced membranes from hepatocytes after cessation of treatment. *J. Cell Biol.* **56**:746.
12. LUFT, J. H. 1961. Improvements in epoxy resin embedding methods. *J. Biophys. Biochem. Cytol.* **9**:409.
13. REYNOLDS, E. S. 1963. The use of lead citrate at high pH as an electron-opaque stain in electron microscopy. *J. Cell Biol.* **17**:208.
14. WEIBEL, E. R., and R. P. BOLENDER. 1973. Stereological techniques for electron microscopic morphometry. *In* Principles and Techniques of Electron Microscopy. Vol. 3. M. A.

Hayat, editor. Van Nostrand Reinhold Company, New York. 237.

15. WEIBEL, E. R. 1969. Stereological principles for morphometry in electron microscopic cytology. *Int. Rev. Cytol.* **26**:235.
16. DIXON, W. J., and F. J. MASSEY. 1957. Introduction to Statistical Analysis. McGraw-Hill Book Company, New York.
17 WEIBEL, E. R., W. STÄUBLI, H. R. GNÄGI, and F. A. HESS. 1969. Correlated morphometric and biochemical studies on the liver cell. I. Morphometric model, stereologic methods, and normal morphometric data for rat liver. *J. Cell Biol.* **42**:68.
18. WEIBEL, E. R., G. S. KISTHER, and W. F. SCHERLE. 1966. Practical stereological methods for morphometric cytology. *J. Cell Biol.* **30**:23.
19. GIGER, H., and H. RIEDWYL. 1970. Bestimmung der Grössenverteilung von Kugeln aus Schnittkreisradien. *Biom. Z.* **12**:156.
20. SCHERLE, W. 1970. A simple method for volumetry of organs in quantitative stereology. *Mikroskopie.* **26**:57.
21. GLAGOLEFF, A. A. 1933. On the geometrical methods of quantitative mineralogic analysis of rocks. *Tr. Inst. Econ. Minine Metal.* 59.
22. WEIBEL, E. R. 1972. Current capabilities and limitations of available stereological techniques. II. Point counting methods. *In* Stereology 3. E. R. Weibel, G. Meek, B. Ralph, P. Echlin, and R. Ross, editors. Blackwell Scientific Publications, Oxford. 367.
23. HILLIARD, J. E., and J. W. CAHN. 1961. An evaluation of procedure in quantitative metallorgraphy for volume-fraction analysis. *Trans. Am. Inst. Mining Eng.* **221**:344.
24. HILLIARD, J. E. 1965. *In* Recrystallization, Grain Growth and Textures. The American Society for Metals, Metals Park, Ohio. 267.
25. AMSTERDAM, A., M. SCHRAMM, I. OHAD, Y. SALOMON, and Z. SELINGER. 1971. Concomitant synthesis of membrane protein and exportable protein of the secretory granule in rat parotid gland. *J. Cell Biol.* **50**:187.
26. FAWCETT, D. W. 1962. Physiologically significant specializations of the cell surface. *Circulation.* **26**:1105.
27. GEUZE, J. J., and C. POORT. 1973. Cell membrane resorption in the rat pancreas cell after in vivo stimulation of the secretion, as studied by in vitro incubation with extracellular space markers. *J. Cell Biol.* **57**:159.
28. BOLENDER, R. P. 1974. Stereology applied to structure-function relationships in pharmacology. *Fed. Proc.* In press.